YMTHE, Volume *32*

Supplemental Information

TALEN-edited allogeneic inducible dual CAR T cells enable effective targeting of solid tumors while mitigating off-tumor toxicity

Sonal Dharani, Hana Cho, Jorge Postigo Fernandez, Alexandre Juillerat, Julien Valton, Philippe Duchateau, Laurent Poirot, and Shipra Das

Supplemental Material

Supplemental Figures

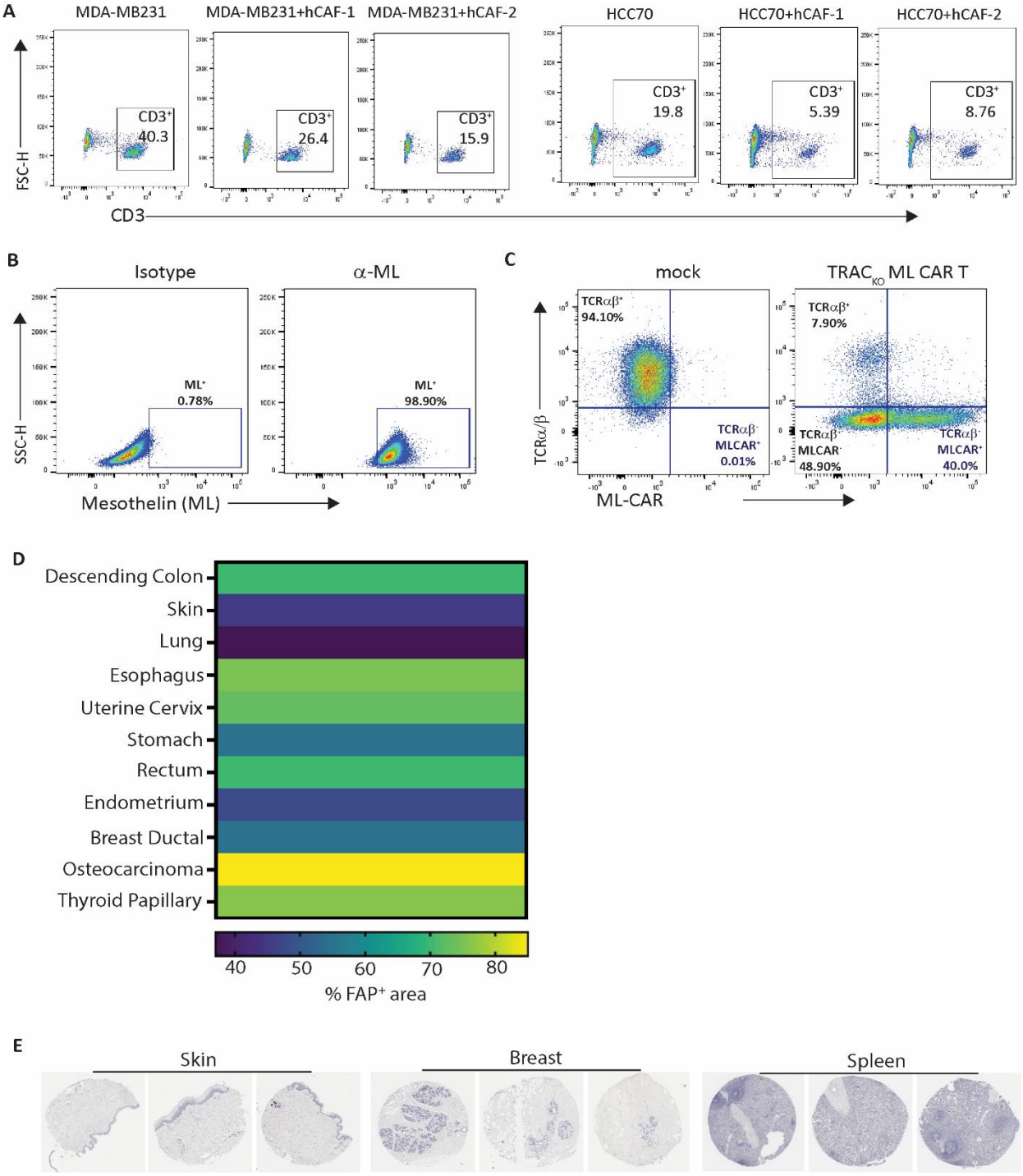

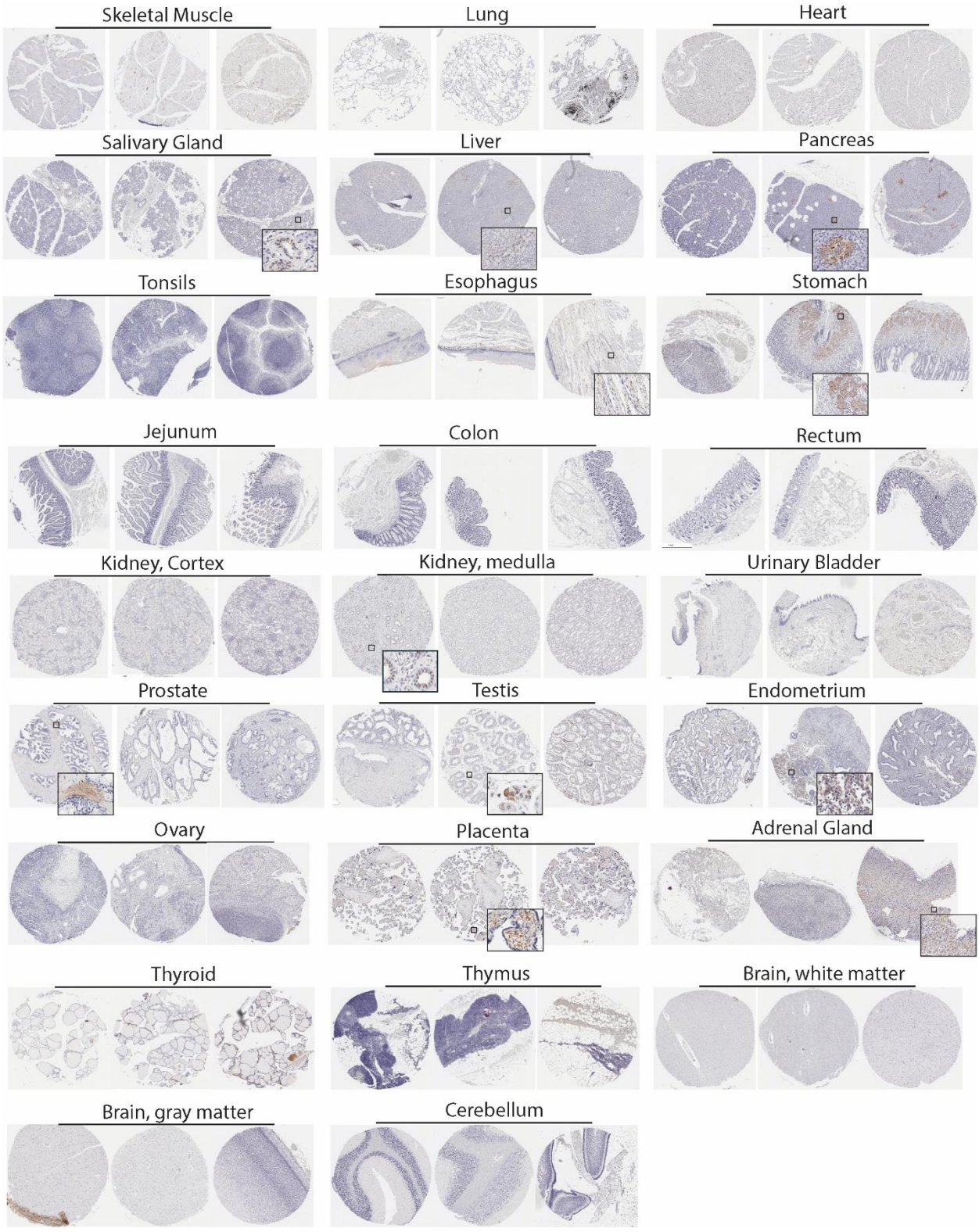

Figure S1. FAP^{+} CAFs are restricted to tumor microenvironment and inhibit intra-tumor T cell infiltration and CAR T-cell activity

(**A**) Flow cytometry plots representing infiltrated T cells in spheroids of MDA-MB-231 and HCC70 tumor cells, either alone or co-cultured with TNBC patient-derived CAFs. (**B**) Analysis of Mesothelin (ML) expression on surface of MDA-MB-231-Luc tumor cells, as determined by flow cytometry. (**C**) Heatmap depicting percentage positive area stained for human FAP protein in immunohistochemical analysis of patient tumor tissue microarray, corresponding to **Figure 1E**. (**D)** Flow cytometry plot depicting ML CAR expression in mock transduced and $TRAC_{KO}$ MLCAR T-cells. (**E**) Immunohistochemical analysis of healthy donor tissue microarray for FAP protein detection. Inlays represent 40X magnification of positively stained area.

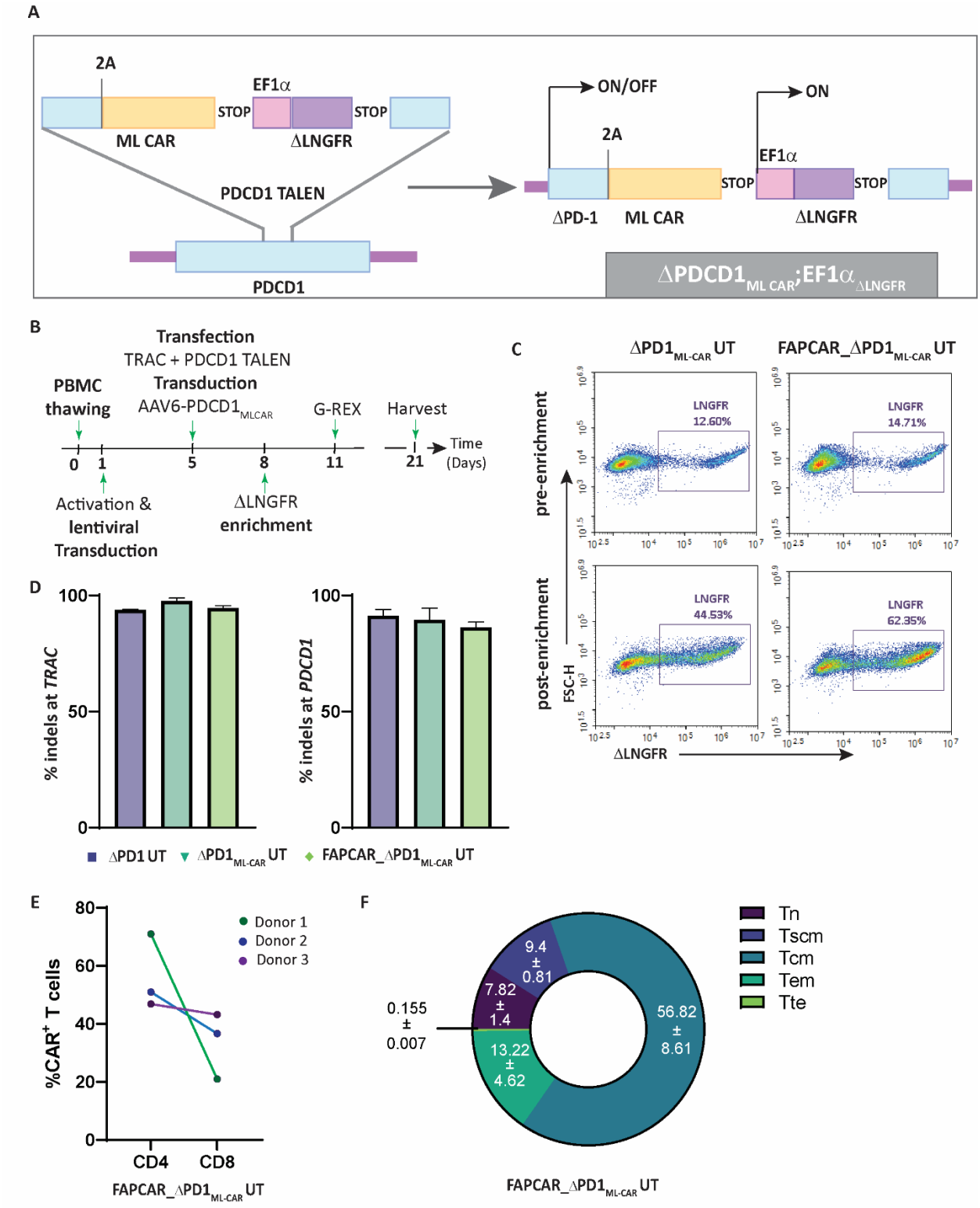

Figure S2. Multiplex engineering of T cells using TALEN mediated gene editing and AAV6 DNA donor template integration

(**A**) Schematic showing structure of the DNA repair matrix for disruptive insertion at PDCD1, consisting of ML CAR followed by *PDCD1* independent, EF1α promoter-driven ΔLNGFR transgene as marker for successful integration and subsequent enrichment. (**B**) Experimental strategy for TALEN-mediated gene editing, lentiviral and AAV6 transduction, ΔLNGFR enrichment by MACS and expansion of engineered human universal CAR T-cells. (**C**) Flow cytometry plots depicting ΔLNGFR expression pre- and post- enrichment of genetically modified UT cells. **(D)** Frequencies of insertions and deletions (indels) obtained by high-throughput DNA sequencing of TRAC (left) and PDCD1 (right) TALEN cut-site, obtained from indicated engineered T-cells (n=2 donors). **(E)** Frequency of $CD4^+$ and $CD8^+$ cells gated on $FAPCAR^+$ subpopulation of FAPCAR_$\Delta PD1_{MLCAR}$ UT-cells at end of engineered T cell expansion. Bars show the means ± SD, n=3. **(F)** Frequency of $CD62L^+CD45RA^+CD45RO^-$ (T_N naive), $CD62L^+CD45RA^+$ $CD45RO^+$ (T_{SCM} stem central memory), $CD62L^+CD45RA^-$ $CD45RO^+$ (T_{CM} central memory), $CD62L^-CD45RA^-$ $CD45RO^+$ (T_{EM} effector memory) and $CD62L^-CD45RA^+$ $CD45RO^-$ (T_{TE} terminal effector) gated on $FAPCAR^+$ subpopulation of FAPCAR_$\Delta PD1_{MLCAR}$ UT-cells post engineering. Values indicate means ± SD, n=2.

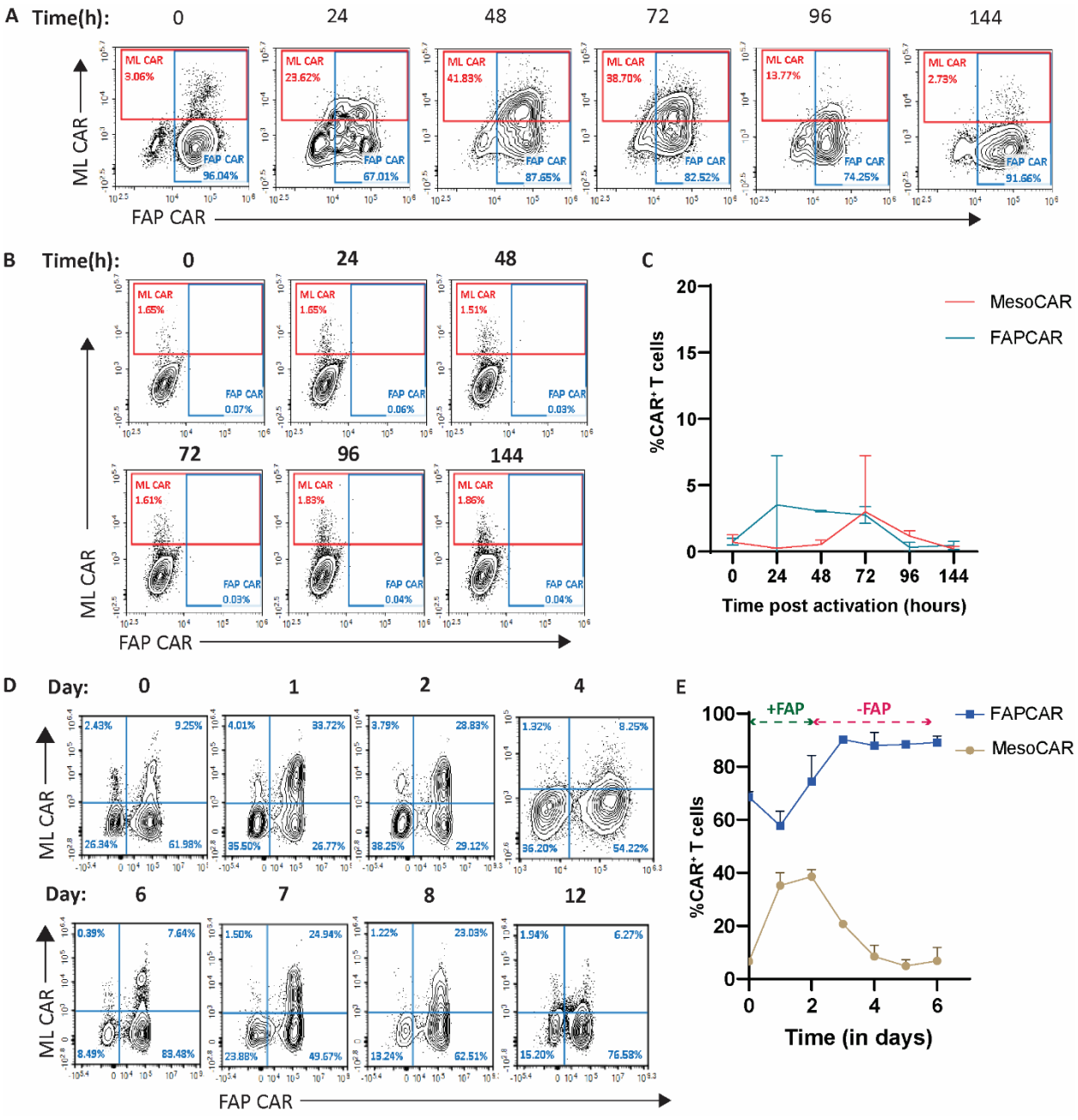
A
Time(h):
0
24
48
72
96
144
ML CAR
FAP CAR
ML CAR 3.06%
FAP CAR 96.04%
ML CAR 23.62%
FAP CAR 67.01%
ML CAR 41.83%
FAP CAR 87.65%
ML CAR 38.70%
FAP CAR 82.52%
ML CAR 13.77%
FAP CAR 74.25%
ML CAR 2.73%
FAP CAR 91.66%
B
Time(h):
0
24
48
72
96
144
ML CAR
FAP CAR
ML CAR 1.65%
FAP CAR 0.07%
ML CAR 1.65%
FAP CAR 0.06%
ML CAR 1.51%
FAP CAR 0.03%
ML CAR 1.61%
FAP CAR 0.03%
ML CAR 1.83%
FAP CAR 0.04%
ML CAR 1.86%
FAP CAR 0.04%
C
MesoCAR
FAPCAR
%CAR+ T cells
Time post activation (hours)
D
Day:
0
1
2
4
6
7
8
12
ML CAR
FAP CAR
2.43%
9.25%
26.34%
61.98%
4.01%
33.72%
35.50%
26.77%
3.79%
28.83%
38.25%
29.12%
1.32%
8.25%
36.20%
54.22%
0.39%
7.64%
8.49%
83.48%
1.50%
24.94%
23.88%
49.67%
1.22%
23.03%
13.24%
62.51%
1.94%
6.27%
15.20%
76.58%
E
+FAP
-FAP
FAPCAR
MesoCAR
%CAR+ T cells
Time (in days)

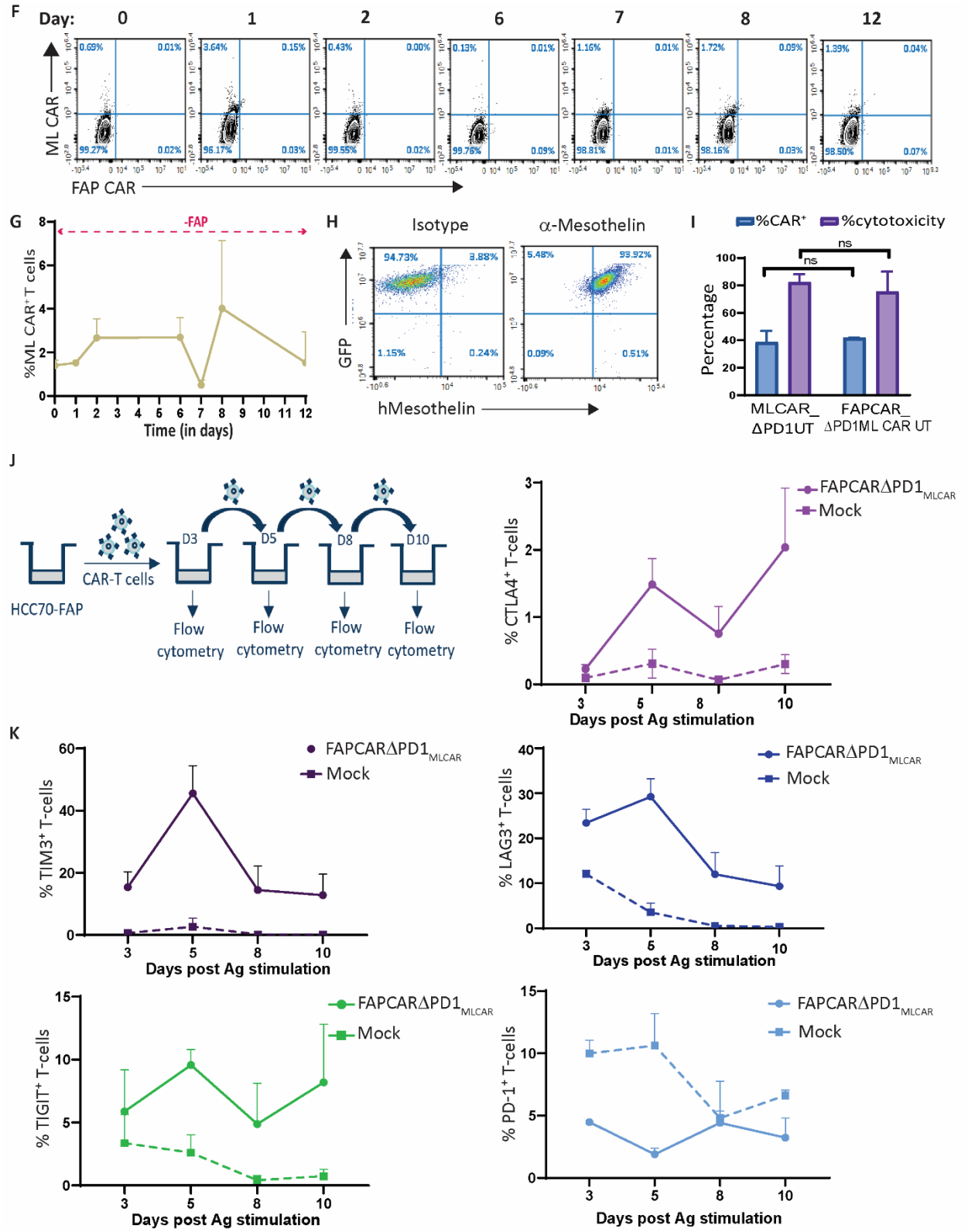

Figure S3. FAP CAR-mediated regulation of *PDCD1* integrated ML CAR expression and activity

(**A**) Flow cytometry plots depicting kinetics of ML CAR surface expression on FAPCAR_ΔPD1$_{ML\ CAR}$ UT cells following FAP CAR activation with FAP protein incubation. (**B**) Flow cytometry plots depicting kinetics of ML CAR surface expression on control ΔPD1$_{ML\ CAR}$ UT cells following FAP protein incubation. (**C**) Graph depicting kinetics of FAP CAR and ML CAR expression following FAP protein incubation of control ΔPD1$_{ML\ CAR}$ UT-cells. Each data point represents mean ± SD, n=3 donors. (**D**) Representative flow cytometry plots time course of FAP CAR and MLCAR expression upon FAP CAR stimulation and withdrawal of stimulus (FAP protein) from FAPCAR_ΔPD1$_{ML\ CAR}$ UT-cells. (**E**) Graph representing time course of FAP CAR and MLCAR expression upon FAP CAR stimulation and withdrawal of stimulus (FAP protein) from FAPCAR_ΔPD1$_{ML\ CAR}$ UT-cells. Each data point represents mean ± SD, n=2 donors. (**F**) Flow cytometry plots representing time course of FAP CAR and MLCAR expression upon stimulation and withdrawal of stimulus (FAP protein) from control ΔPD1$_{ML\ CAR}$ UT-cells. (**G**) Graph representing time course of MLCAR expression without FAP CAR stimulation (with FAP protein) of FAPCAR_ΔPD1$_{ML\ CAR}$ UT-cells. Each data point represents mean ± SD, n=3 donors. (**H**) Analysis of ML expression on surface of NCI-H226-GFP-Luc tumor cells, as determined by flow cytometry. (**I**) Bar graph representing percentage MLCAR positive cells in two engineered UT cell populations-MLCAR_ΔPD1 and FAPCAR_ΔPD1ML CAR cells 48 h post FAP-activation, with their corresponding cytotoxic activity against ML^{+}FAP^{-} NCI-H226-LUC tumor cells co-incubated for 24 h, with target cells at Effector: Target ratio=1:1. Bars show the means ± SD, n=2; P-values determined by Student t test (two-tailed, unpaired), ns-not significant. (**J**). Schematic of serial stimulation of FAPCARΔPD1$_{MLCAR}$ UT-cells with FAP-transduced ML^{+} HCC70 cells over a period of 10 days. **(K**) Graph depicting kinetics of exhaustion marker expression as measured by flow cytometry analysis on Mock transduced or FAPCARΔPD1$_{MLCAR}$ UT-cells, serially stimulated with FAP+ML+ HCC70 cells over 10 days. Each data point represents mean ± SD, n=2 donors.

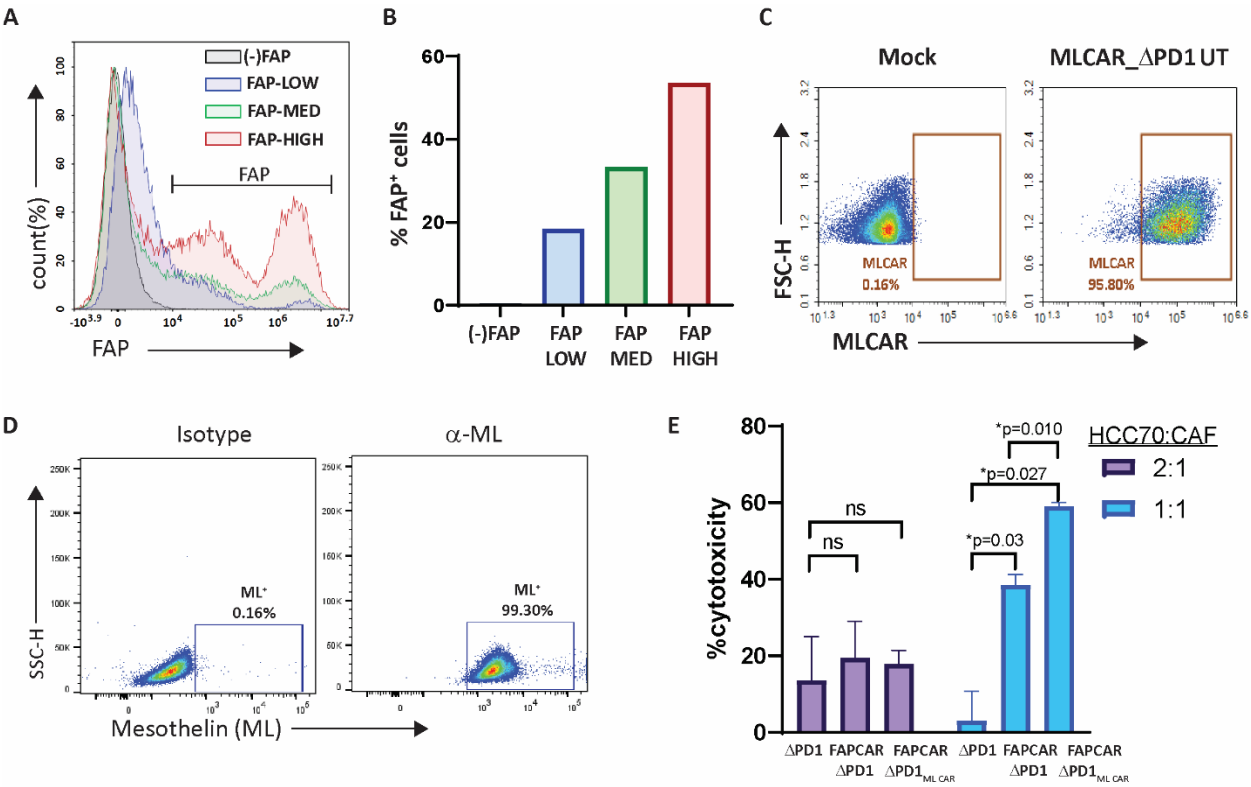

Figure S4. FAPCAR_ΔPD1$_{ML\ CAR}$ UT-cells efficiently target FAP$^+$ML$^+$tumors in a FAP CAR activation-dependent manner

(**A**) Flow cytometry histogram depicting expression of FAP in (-)FAP, FAP(LOW), FAP(MED) and FAP(HIGH) NCI-H226-Luc transduced cells. (**B**) Graph depicting percentage of FAP$^+$ cells in the different NCI-H226-Luc cells, as indicated. (**C**) Flow cytometry plot depicting ML CAR expression in mock transduced and MLCAR_ΔPD1 UT-cells. (**D**) Analysis of ML expression on HCC70-Nanoluc tumor cells, as determined by flow cytometry. (**E**) Bar graph representing percentage HCC70-GFP tumor cell lysis post cytotoxicity assay of indicated engineered T-cells against HCC70 and CAF spheroid co-cultures at ratios of 2:1 and 1:1 and at Effector: Target ratio of 5:1. Data representative of n=2 independent experiments, 2 donors per experiment, 3 technical replicates per donor per experiment. Bars show the means ± SD; P- values determined by Student t test (two-tailed, unpaired). ns-not significant, *p≤0.05.

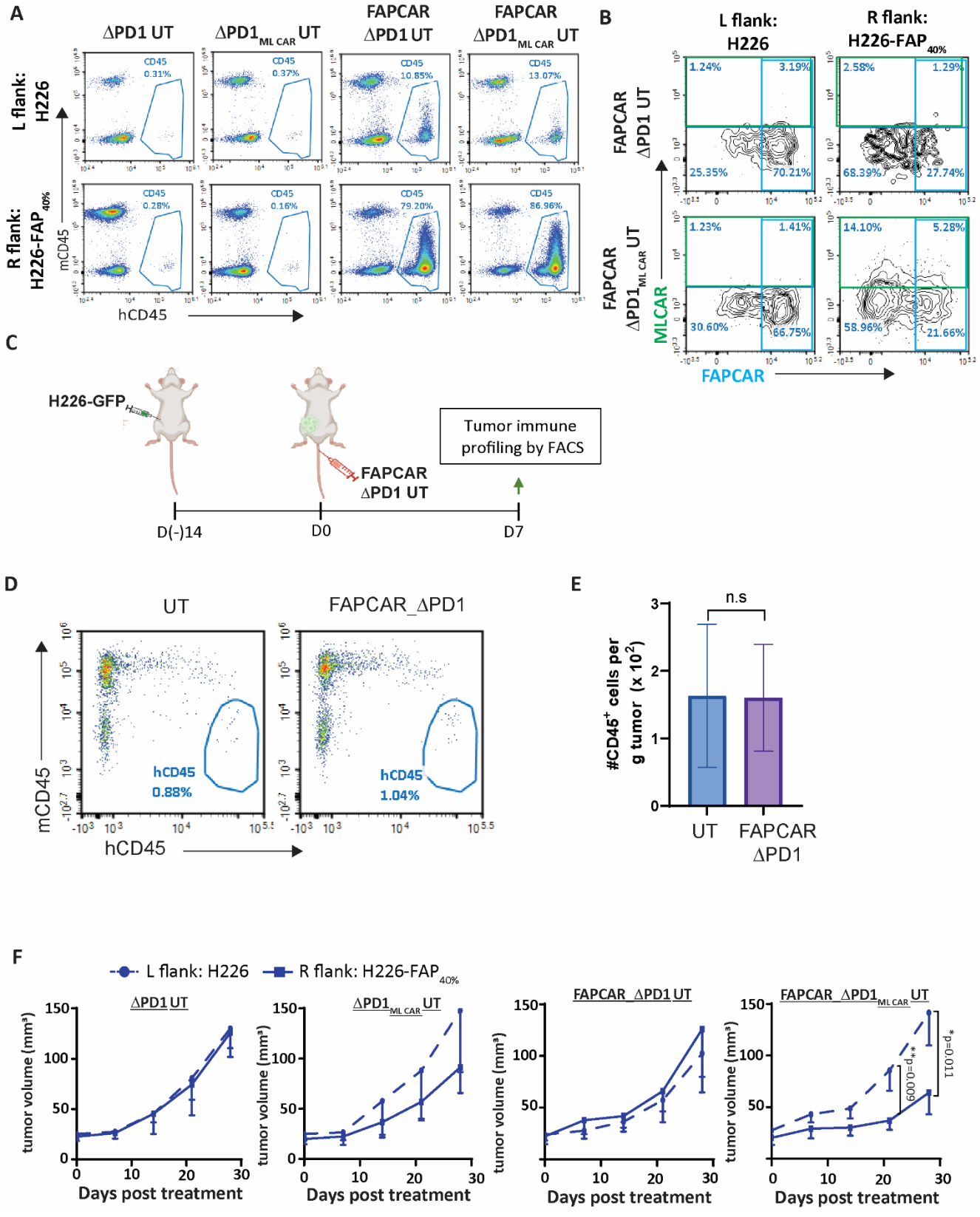
A
ΔPD1 UT
ΔPD1ML CAR UT
FAPCAR ΔPD1 UT
FAPCAR ΔPD1ML CAR UT
L flank: H226
R flank: H226-FAP40%
CD45 0.31%
CD45 0.37%
CD45 10.85%
CD45 13.07%
CD45 0.28%
CD45 0.16%
CD45 79.20%
CD45 86.96%
mCD45
hCD45
B
L flank: H226
R flank: H226-FAP40%
FAPCAR ΔPD1 UT
FAPCAR ΔPD1ML CAR UT
1.24%
3.19%
25.35%
70.21%
2.58%
1.29%
68.39%
27.74%
1.23%
1.41%
30.60%
66.75%
14.10%
5.28%
58.96%
21.66%
MLCAR
FAPCAR
C
H226-GFP
FAPCAR ΔPD1 UT
Tumor immune profiling by FACS
D(-)14
D0
D7
D
UT
FAPCAR_ΔPD1
hCD45 0.88%
hCD45 1.04%
mCD45
hCD45
E
n.s
#CD45+ cells per g tumor (x 10^2)
UT
FAPCAR ΔPD1
F
L flank: H226
R flank: H226-FAP40%
ΔPD1 UT
ΔPD1ML CAR UT
FAPCAR_ΔPD1 UT
FAPCAR_ΔPD1ML CAR UT
tumor volume (mm³)
Days post treatment
6000=d**
*p=0.011

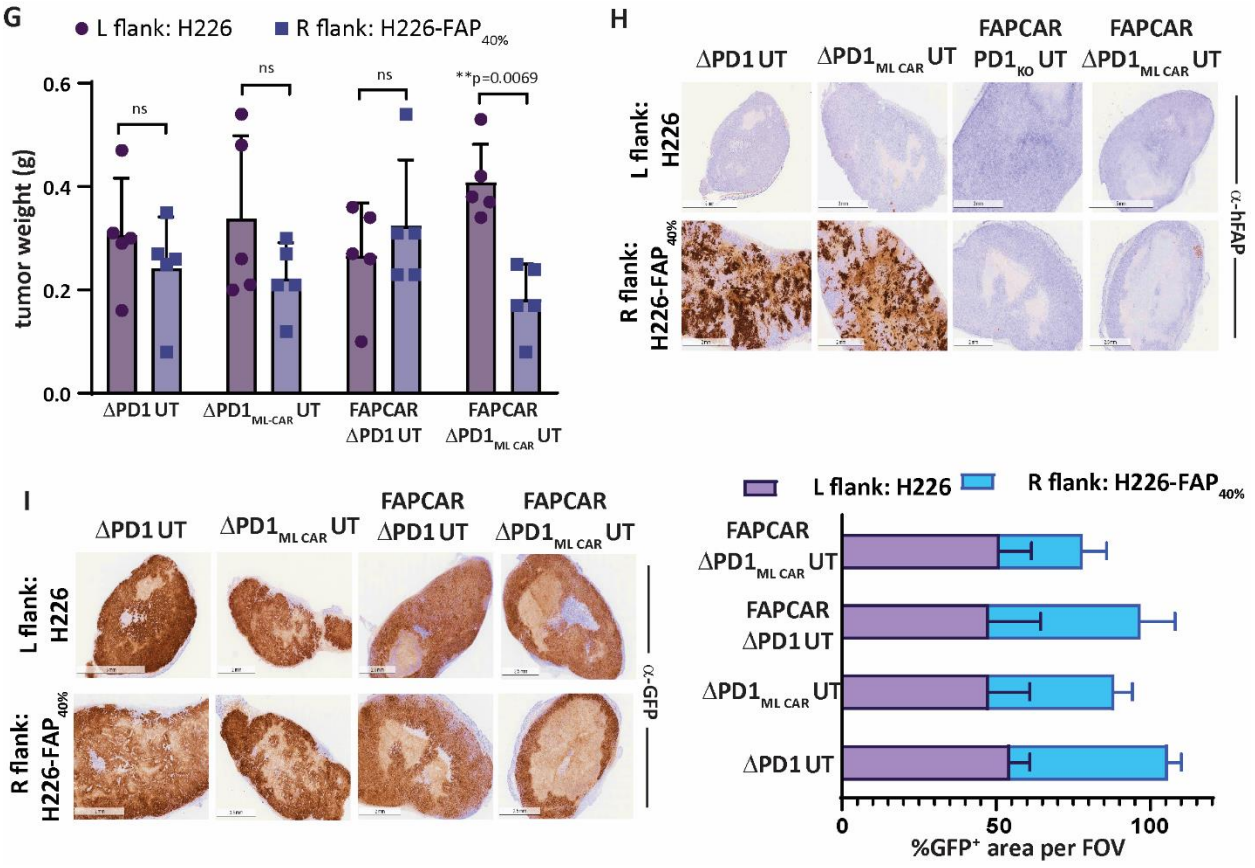

Figure S5. FAPCAR_ΔPD1ML CAR UT-cells display enhanced anti-tumor activity with no detectable 'off tumor' toxicity.

(**A**) Flow cytometry plot of human CD45$^+$ UCAR T-cell population in subcutaneous tumors harvested from mice treated as indicated. (**B**) Flow cytometry plot of percentage of FAP CAR$^+$ and ML CAR$^+$ among viable human CD45$^+$ UT cells in subcutaneous tumors harvested from mice treated as indicated. (**C**) Schematic of UCAR T-cell treatment and analysis of subcutaneous H226 tumor implanted in NSG mice. (**D**) Flow cytometry plot of human CD45+ UCAR T-cell population in subcutaneous H226 tumors harvested from mice treated as indicated. (**E**) Bar graph representing quantitation of total number of hCD45+ cells per gram tumors from mice treated with indicated UT-cells 7 days post administration, as determined by flow cytometry. P-values determined by Student t test (two-tailed, paired), n=2 mice per cohort. ns-not significant. (**F**) Graphs indicating comparative growth kinetics of left flank H226 tumors and right flank H226-FAP$_{40\%}$ tumors, treated with indicated UT cells. Each point represent mean ± s.d, n= 3 mice per cohort; ; P-values determined by Student *t* test (two-tailed, paired). *p≤0.05, **p≤0.01. (**G**) Graph depicting weight

in grams of tumors excised from different cohorts at study endpoint, as indicated. Each bar represent mean ± s.d, n= 3-5 mice per cohort; ; P-values determined by Student *t* test (two-tailed, paired), ns-not significant, **p≤0.01. (**H**) Representative images of immunohistochemical analysis for FAP expression on excised tumors treated as indicated. (**I**) Representative images of immunohistochemical analysis for GFP expression on excised tumors treated as indicated. On the right, stacked bar graph representing quantitation of percentage GFP^+ area corresponding to IHC samples in the left panel. Each bar represents mean ± s.d of at least four field of views per tumor, n=3-5 mice per cohort.

Table S1. Percentage FAP^+ area in tissue microarray of tumor biopsy tissues, as determined by immunohistochemistry.

Tumor tissue	%FAP^+ stained area
Descending Colon	70.0
Skin	45.0
Lung	37.0
Esohagus	75.0
Uterine Cervix	75.0
Stomach	73.0
Rectum	55.0
Endometrium	47.80
Breast Ductal	55.0
Osteocarcinoma	85.0
Thyroid Papillary	76.0

Table S2. Percentage FAP^+ area in tissue microarray of normal tissues from three healthy donors, as determined by immunohistochemistry.

	% FAP^+ stained area		
Healthy Tissue	**Donor-1**	**Donor-2**	**Donor-3**
Skin	3.0829	2.9635	0.9712
Breast	0.6396	2.4834	1.2601
Spleen	0.3186	0.3245	0.2801
Skeletal muscle normal	12.4789	3.2692	0.2935
Lung normal	19.3374	0.2515	1.1241
Liver normal	2.3799	3.49	0.8303
Stomach, body normal	11.7077	13.0123	14.6087
Colon normal	0.376	1.0094	0.3449
Kidney, cortex	0.9469	0.6967	0.2909
Kidney, medulla	3.2297	0.4884	0.3914
Prostate normal	0.1076	1.3936	0.5353
Placenta normal	20.2895	11.3175	15.6667
Brain, white matter	0.2122	0.1951	0.0159
Brain, gray matter	0.064	0.1807	0.0332
Cerebellum	0.09	0.1053	0.7169
Lymph node	0.2464	0.285	0.7432
Heart	2.0957	1.2655	3.2937
Salivary gland	1.0228	0.2064	0.8257
Pancreas	1.3192	1.8801	2.3008
Tonsil	0.0377	0.0704	0.0571
Esophagus	4.4227	5.7468	1.5048
Small intestine, jejunum	0.3714	0.3292	0.2483
Rectum	0.1932	1.42	0.6689

Urinary bladder	1.8392	1.488	2.0712
Testis	0.6519	3.2515	7.5429
Endometrium	8.0456	5.8058	1.6278
Ovary	0.2577	0.1324	0.3867
Adrenal gland	5.6342	11.4769	13.5404
Thyroid	2.9673	4.8813	12.22
Thymus	0.9455	1.078	3.7831